Infrared Spectral, Structural, and Conformational Studies of Zwitterionic L-Tryptophan

Xiaolin Cao and Gad Fischer*

Department of Chemistry, The Faculties, The Australian National University, Canberra, ACT 0200, Australia

Received: July 15, 1999; In Final Form: September 10, 1999

The infrared spectrum, molecular structure, and conformations of L-tryptophan in isolated zwitterionic form have been studied by means of a recently developed infrared sampling technique and ab initio molecular orbital calculations using a nonaqueous self-consistent reaction field (SCRF). A complete mid-IR spectrum of monomeric tryptophan in zwitterionic form was obtained in a solid solvent of KBr. SCRF calculations using KBr as the continuum at the HF/6-31G(d,p) level were performed on zwitterionic tryptophan to predict its structure and vibrational frequencies. Three possible conformers were found, and one of them was identified to be predominant in the prepared sample on the basis of spectral and energy comparisons. Good agreement in terms of both frequencies and intensities was established between the calculated and observed infrared spectra. The detailed molecular structure of the predominant conformer of zwitterionic tryptophan was predicted and discussed.

Introduction

The naturally occurring amino acid L-tryptophan (Trp) has been used as a fluorescence probe to monitor protein conformations and dynamics,[1−3] and hence the electronic spectra of Trp and its derivatives have been the subject of intense investigation for the past two decades. In particular, studies of the electronic spectroscopy of these species in molecular beams have been carried out by the groups of Levy[4−12] and Sulkes.[13−16] The nonexponential fluorescence decay of Trp in aqueous solutions is not completely understood, although the proposal that the emission is from noninterconverting rotamers which have different lifetimes due to different rates of intramolecular charge transfer is now widely accepted.[5−7,17,18] For the zwitterion, conformational calculations have suggested the existence of six low-energy conformations.[3,19] NMR results for Trp in solution have been analyzed in terms of these six low-energy conformations, and the g^- conformer was found to be the dominant species.[20] This contrasts the g^+ conformation, found for tryptophan hydrochloride in the crystal.[21] In the electronic excitation, and resonance-enhanced two-photon ionization spectra of jet-cooled Trp, corresponding to the neutral unionized monomer,[5] six peaks have been identified and assigned to different stable conformers of this molecule in the ground electronic state.[5−7] No evidence for the existence of multiple conformers has been reported in Raman spectroscopy.[22−26] Because of the limitations of existing infrared sampling techniques, very few infrared studies have been carried out to study conformations of zwitterionic Trp.

Fourier transform infrared (FTIR) spectroscopy and ab initio molecular orbital calculations of potential energy surfaces are powerful methods for the study of molecular structures, conformations, and molecular vibrations. A number of ab initio molecular orbital calculations on amino acids have been reported.[27−32] Most calculations were performed on the unionized neutral species using SCF methods, applicable to isolated molecules but not to aqueous solutions or KBr pellet spectra. In aqueous solutions and in the solid state, Trp is present as the zwitterion, while in the vapor (isolated molecule) it occurs as the neutral unionized molecule.[5] In our previous ab initio calculations on alanine[33] and phenylalanine,[34] it was noted that the isolated zwitterions are unstable. Standard SCF (for isolated molecules) calculations performed on zwitterionic amino acids always converge to the unionized neutral structure ($H_2N-CHR-CO_2H$), or to a structure with strong intramolecular hydrogen bonding, structures not representative of the amino acids in the solid state or in aqueous solutions.

Accordingly, we proposed a new methodology for the study of IR spectra and for carrying out ab initio calculations of zwitterionic amino acids ($H_3N^+-CHR-CO_2^-$, R side chain). This approach allows for measurement of the IR spectra of largely monomeric zwitterions and for undertaking ab initio calculations appropriate to monomeric zwitterions. Ab initio calculations of amino acid zwitterions must take into account the stabilizing influence of the near environment. Self-consistent reaction field (SCRF) calculations do this. Several SCRF calculations (for solvated molecules) have been performed on zwitterionic amino acids using water as the solvent.[35−37] However, SCRF calculations that use water as the continuum are subject to error, because water molecules engage in very strong hydrogen bonding with the solute molecules and hence specific intermolecular interactions should be included.[38,39] To compound the problem of matching calculated with observed spectra, complete and resolved infrared spectra of amino acids in aqueous solution are difficult to obtain because of the strong absorption of water molecules. Thus, no fully satisfactory aqueous solution spectra are available and the aqueous SCRF calculated spectra suffer from shortcomings, making a comparison between the two not particularly meaningful.

For the measurement of IR spectra of largely monomeric zwitterions of amino acids a dissolution−spray−deposition (DSD) procedure has been developed.[33,34] It does not require sample evaporation and so is not subject to the problems of sample decomposition. The key idea of this new technique involves separation and isolation of the sample molecules using a solid solvent. With this method, amino acids are trapped and

* Corresponding author. E-mail: Gad.Fischer@anu.edu.au. Fax: +61 2 6249 0760. Phone: +61 2 6249 2935.

10.1021/jp992421c CCC: $18.00
Published on Web 11/04/1999

separated in an alkali halide solid solvent but still exist in zwitterionic form.

The theoretical problem of matching calculation with experiment has been largely overcome as a consequence of the new sampling technique. Meaningful self-consistent reaction field (SCRF) calculations can be undertaken for molecules trapped in a matrix, provided the continuum approach satisfactorily describes the solute−solvent intermolecular interactions. Since in the DSD prepared sample the zwitterions of amino acid are trapped and separated in a solid solvent of an alkali halide (KBr), we consequently use KBr solid solvent as the continuum for the SCRF calculations. Unlike the very polar solvent water, with a large dielectric constant ($\epsilon = 78.54$,[40] 25 °C), the solid solvent KBr has a much smaller dielectric constant ($\epsilon = 4.88$[40]). It is argued that for an alkali halide matrix such as KBr the continuum model may be used to describe the solvation effect.

The infrared spectra, molecular structures, and conformations of a set of zwitterionic amino acids with nonpolar side chains, such as glycine (Gly),[41] alanine (Ala),[33] phenylalanine (Phe),[34] leucine (Leu),[42] isoleucine (Ile),[42] and methionine (Met)[42] have been studied with the above-mentioned approach. For this set of amino acids, our studies have shown that the reaction field effect is concentrated predominantly on the main chains ($H_3N^+-CHR-CO_2^-$) and not the side chains (R). Therefore, similarities can be expected, and are found, in the IR spectra and molecular structures among these amino acids. Here, we report results on the IR spectra of zwitterionic Trp and on the calculated structures of a number of its conformations.

Experimental Section

Details of the preparation of a DSD sample of Trp have been described elsewhere.[33] In brief, a DSD sample is obtained by spraying a solution (aqueous) of sample (Trp) and matrix (KBr) onto an IR transparent window (pure KBr pellet) and subsequently removing the solvent (water) by evaporation under preset favorable conditions. When the solvent is evaporated completely, only the KBr matrix together with trapped and isolated sample molecules remain on the window. By this procedure, the matrix isolation of zwitterionic amino acids can be achieved without the requirement of sample evaporation. Conditions of the deposition are similar to those used for Phe.[34] The mass ratio of KBr (FT-IR grade, Aldrich) and Trp (ICN) used for this study was chosen to be 80. The deposition temperature on the window was about 78 °C.

When the deposition was deemed complete, the window with its deposit was placed in a sample cell for measurement. The sample cell was mounted in an FTIR spectrometer (IFS66, Bruker), and both the spectrometer and sample cell were purged continuously by dry nitrogen gas. The DSD spectra of Trp were recorded at a resolution of 4 cm^{-1} in the full mid-IR range (4000−400 cm^{-1}). For comparison, the normal KBr pellet spectrum was also recorded at the same resolution. Despite the low absorbances measured and the background subtraction process,[33] the level of noise in the spectra was comparable to that encountered in the measurement of normal KBr pellet spectra.

It should be noted that the function of the KBr in the DSD method, is essentially different from that in the KBr pellet method. For the latter, the KBr is mainly a supporting host and the solid sample molecules cannot be separated at the molecular level by mechanical grinding and mixing. On the other hand, in the DSD method, the KBr behaves as a matrix in which the sample molecules are isolated as monomers. Therefore, for this purpose, other materials and, in particular, other alkali halides (infrared transparent) can also be used as potential matrices.

Trp is characterized by a relatively high melting point, 282 °C, and, compared with most other amino acids, a relatively low aqueous solubility, 0.012 g/g of water.[40] As good single crystals are difficult to obtain, only its space group and unit cell dimensions from X-ray powder scattering patterns[43] have been reported. The detailed molecular structure of zwitterionic Trp has not been found in the literature.

Calculations

It was pointed out above that zwitterionic amino acids do not exist as isolated monomers. To carry out meaningful calculations on the zwitterionic forms of the amino acids, either solvation effects or specific intermolecular interactions must be included. Calculations including specific intermolecular interactions are usually impracticable, because of the number of molecules (large multimers or clusters) that must be included in the computation. However, the inclusion of a general solvation effect in the calculations can be readily undertaken. SCRF methods,[38] which are implemented in the Gaussian packages, include the solvation effect. These methods all model the solvent as a continuum of uniform dielectric constant, the reaction field, which can interact with the solute molecules and lead to net stabilization.

Here, we report SCRF ab initio molecular orbital calculations on Trp at the level HF/6-31G(d,p) of GAUSSIAN 98,[44] using KBr as the continuum. Single-point energy calculations at the SCRF/HF optimized geometries were also carried out at the MP2/6-31G(d) level. The Onsager dipole−sphere model was used. It is specified by two parameters: the dielectric constant, ϵ, of the continuum and the radius, a_0, of the cavity occupied by the solute. In all of our SCRF calculations, only the Onsager model was used, because in this model, the cavity radius can act as a parameter that can be readily adjusted to achieve agreement between the predicted and observed infrared spectra. Furthermore, this model can be used for both full geometrical optimization and vibrational spectra prediction, at two theoretical levels, namely, Hartree−Fock (HF) and density functional theory (DFT). For large molecules (such as Trp), far greater computational resources are required by DFT theory. Moreover, according to our previous SCRF/DFT calculations on Ala, the vibrational spectra predicted by DFT theory did not show better agreement with the DSD spectra than the HF predicted spectra. Therefore, in this study, only SCRF/HF calculations on Trp were performed. It was found that inclusion of polarization functions on the hydrogen atoms is important and has a significant influence on the structure and infrared spectra of zwitterionic amino acids.[30] Hence, in ab initio calculations of zwitterionic amino acids, the polarization functions on hydrogen atoms should be included in the basis set whenever possible.

The dielectric constant of KBr was taken as 4.88, and the cavity radius of Trp was set at 3.45 Å.[34] Started from all the possible conformations, the structures were optimized without imposing any geometrical constraints. Only three different stationary points were found. To verify that these stationary points were indeed local minima, harmonic vibrational frequencies were calculated following the structure optimization, by analytic second differentiation of the energy with respect to nuclear displacements. No imaginary frequencies were found for any of the stationary points. Thus, these three stationary points are all real energy minima and correspond to three different structural conformers. They have been labeled G, G*, and G^+. The first two correspond roughly to the conformations previously labeled g^- (gauche$^-$) perp and g^- anti, respectively.[19] The G^+ conformation has no clear counterpart, but is closest to

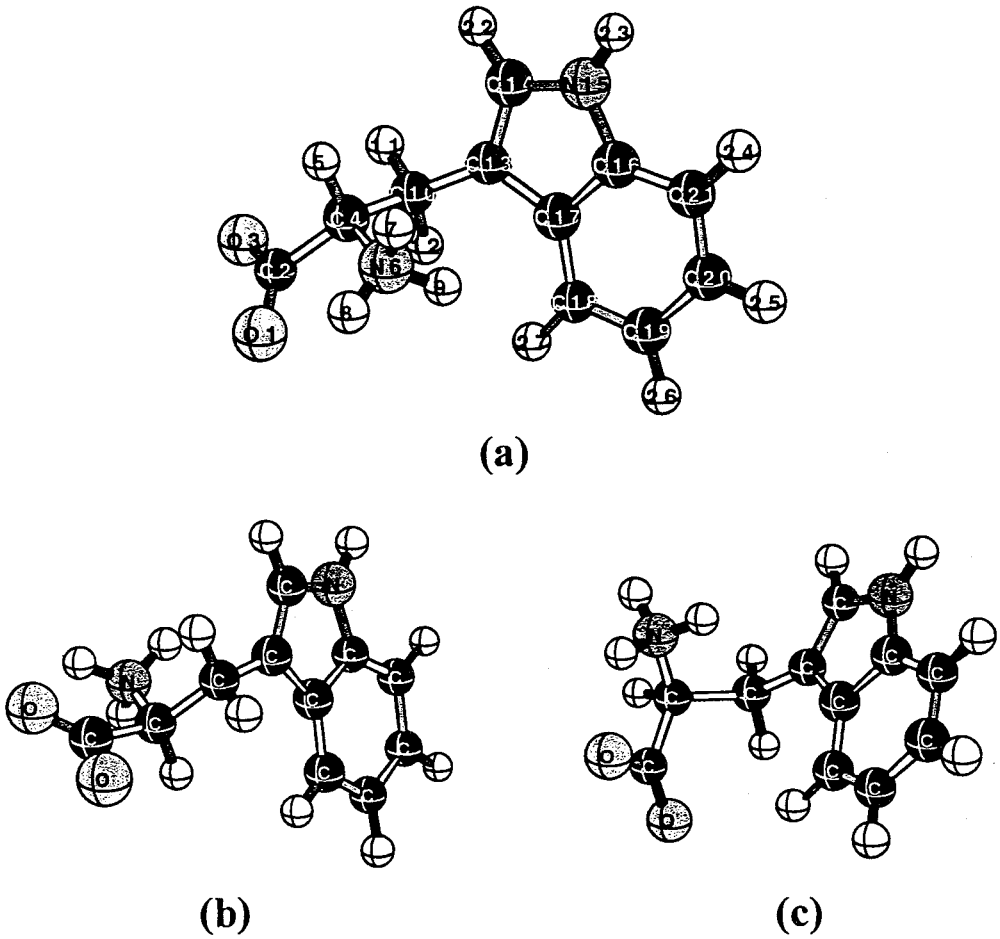

Figure 1. SCRF/HF calculated geometries of zwitterionic Trp: (a) conformer G; (b) conformer G*; (c) conformer G^+.

the g^+ conformation.[19] This is in contrast to the six or more low-energy conformers found in previous semiempirical energy calculations.[3,19] Of the three stable conformers found in this work, one has been determined to be predominant by means of spectral comparisons and will be discussed in detail in the next section. The SCRF/HF calculated vibrational frequencies have been scaled by a single factor of 0.895 for all conformers to correct the well-known systematic 10−12% frequency overestimation.[38,45]

Calculations carried out at the same theoretical level (HF/6-31G(d,p)), but for the isolated neutral molecule, revealed the existence of six major low-energy rotamers, in agreement with the cooled molecular beam work.[5−7] This confirmed the predictive power of the ab initio calculations, at least in-so-far-as the neutral molecule is concerned, and provided support for the validity of the SCRF calculations for the zwitterion. Calculated geometries and rotational constants were determined for these rotamers, but experimental rotational constants are not available.

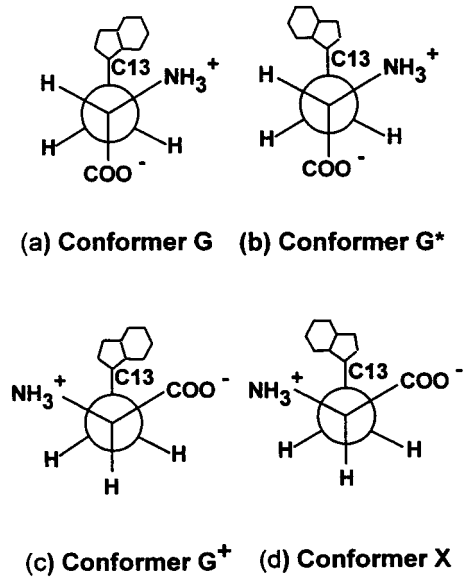

Figure 2. Stereographic projections about the C4−C10 (C_α-C_β) bond of the three predicted Trp conformers G (a), G* (b), G^+ (c), and X-ray structure of Trp·HCl (d).

Results and Discussion

Conformers. The three predicted conformers are labeled according to the relative positions of C13(C_γ) with respect to atom N6 and the orientation of the indole plane. The geometries, drawn to scale, of the three Trp conformers predicted at the SCRF/HF level, are presented in Figure 1. Their stereographic projections about C4−C10 (C_α−C_β) are schematically illustrated in Figure 2 as parts a, b, and c, respectively. For comparison, the X-ray structure of tryptophan hydrochloride salt, Trp·HCl,[21] is also included as Figure 2d. The predicted fundamental vibrational frequencies and intensities in the measurable range (4000−400 cm^{-1}) for all three conformers are tabulated in Table 1, together with the observed DSD band frequencies and intensities. For a direct visual comparison, the DSD spectrum (a) and the "stick" predicted spectra (b, c, d) of conformers G, G*, and G^+, in addition to the KBr pellet spectrum (e), are all presented in Figure 3.

TABLE 1: Vibrational Frequencies (400−4000 cm^{-1}) and Intensities of Zwitterionic L-Tryptophan Obtained by SCRF Calculations[a] and the DSD Method[b]

no.	G^{+a}	G*^{a}	G^{a}	DSD^{b}	assignments^{c}
13	440 (1.2)	424 (1.6)	424 (1.6)	424 (m)	def. R
14	445 (2.0)	446 (3.7)	443 (<1)	453 (vw)	def. r
15	491 (10.2)	495 (5.2)	480 (8.1)	497 (w)	βCO_2^-
16	524 (<1)	519 (<1)	529 (1.1)	529 (vw)	def. r, def. R
				507 (w)	
17	558 (22.1)	559 (12.2)	555 (12.0)	555 (w)	βNH(r)
18	567 (2.4)	560 (2.6)	561 (<1)	n.o.	def. R
19	572 (1.1)	581 (5.6)	574 (4.9)	581 (m)	βNH(r)
20	598 (15.1)	617 (5.9)	609 (6.6)	613 (m)	βCH, βNH(r)
21	639 (<1)	659 (7.2)	642 (1.6)	640 (w)	def. r
22	695 (1.3)	688 (<1)	693 (3.2)	694 (m)	def. r
				660 (w)	
23	738 (2.3)	731 (7.8)	725 (5.3)	n.o.	def. R, def. r
24	744 (15.5)	742 (11.6)	737 (11.6)	740 (s)	βH(R)
25	756 (3.7)	755 (<1)	755 (2.2)	n.o.	βH(R)
26	770 (6.6)	777 (5.2)	774 (4.2)	763 (vw)	βCO_2^-
27	832 (18.5)	810 (5.2)	799 (7.3)	794 (w)	βCO_2^-, βCH_2
28	850 (4.9)	852 (5.0)	850 (1.3)	821 (m)	def. R, def. r
29	863 (<1)	861 (2.9)	860 (1.9)	843 (w)	βH(R)
30	867 (16.3)	867 (1.9)	872 (<1)	n.o.	βH(r)
31	922 (9.6)	879 (40.8)	891 (25.3)	875 (m)	β NH_3^+, βNCC
32	929 (3.5)	921 (5.6)	918 (2.7)	928 (w)	βCH_2
33	959 (2.0)	952 (<1)	955 (<1)	n.o.	βH(R)
34	975 (<1)	988 (1.6)	990 (<1)	n.o.	def. R
35	985 (4.1)	992 (11.3)	1005 (8.8)	1007 (m)	νCN, βNH_3^+
36	992 (3.9)	1024 (<1)	1026 (1.1)	n.o.	βH(R)
37	1042 (23.1)	1025 (<1)	1028 (<1)	n.o.	βH(R)
38	1051 (6.4)	1055 (5.2)	1058 (5.0)	1045 (w)	βNH_3^+
39	1088 (14.6)	1072 (29.6)	1075 (19.1)	1075 (w)	βH(R), βH(r)
40	1093 (3.9)	1084 (9.9)	1086 (6.5)	1100 (m)	βH(r)
41	1104 (5.6)	1113 (<1)	1112 (<1)	n.o.	βH(R)
42	1110 (2.2)	1121 (<1)	1115 (1.8)	1111 (m)	βH(R)
43	1184 (<1)	1181 (<1)	1189 (18.8)	1153 (m)	νCC
44	1216 (5.2)	1204 (7.1)	1203 (4.5)	n.o.	νr
45	1242 (6.0)	1227 (9.8)	1230 (1.2)	1226 (w)	βCH, νR
46	1248 (5.7)	1244 (<1)	1242 (1.2)	n.o.	βCH_2, νr
47	1278 (1.5)	1256 (2.1)	1256 (5.5)	1249 (w)	νR
48	1288 (10.9)	1279 (1.7)	1279 (<1)	1273 (w)	νR, νr
				1283 (w)	
49	1315 (7.5)	1316 (13.9)	1320 (8.4)	1316 (w)	βCH_2, νr
				1302 (w)	
50	1340 (5.4)	1329 (20.8)	1330 (18.1)	1352 (vs)	βCH
51	1347 (9.1)	1341 (16.4)	1340 (<1)	n.o.	βCH, νCC
52	1387 (53.6)	1385 (100)	1385 (88.2)	1388 (vs)	ν_s CO_2^-
53	1419 (90.4)	1408 (13.1)	1411 (10.4)	1407 (sh)	νr
54	1427 (48.2)	1420 (64.4)	1441 (12.1)	1432 (m)	βCH_2
55	1447 (5.7)	1442 (1.1)	1447 (13.2)	1432 (m)	νR
56	1457 (4.2)	1450 (5.9)	1453 (46.1)	1457 (s)	β_s NH_3^+
57	1481 (4.6)	1489 (1.4)	1481 (1.6)	1489 (m)	νR. νr
58	1529 (9.1)	1526 (11.4)	1531 (6.9)	n.o.	νr
59	1579 (<1)	1578 (2.4)	1573 (3.0)	n.o.	νR
60	1584 (7.7)	1595 (6.1)	1600 (6.7)	n.o.	$\beta_{as}NH_3^+$
61	1616 (9.8)	1613 (6.2)	1602 (11.9)	1569 (s)	$\beta_{as}NH_3^+$
62	1624 (1.7)	1623 (4.9)	1619 (4.1)	n.o.	νR
63	1692 (100)	1673 (91.3)	1668 (100)	1625 (vvs)	ν_{as} CO_2^-
64	2880 (3.6)	2839 (16.0)	2844 (8.3)	2840 (vw)	νCH_2
				2816 (vw)	
65	2904 (11.7)	2891 (5.6)	2903 (4.4)	2869 (w)	νCH, νCH_2
66	2924 (39.0)	2928 (17.7)	2905 (15.5)	2906 (m)	νCH(R)
67	2927 (<1)	2955 (3.8)	2918 (9.6)	2934 (w)	νCH, νCH_2
68	2986 (19.2)	2997 (9.6)	3002 (6.6)	2975 (w)	νCH(R)
69	2995 (7.4)	3014 (2.1)	3012 (2.4)	3004 (w)	νCH(R)
70	3020 (1.4)	3030 (2.2)	3030 (2.7)	3070 (w)	νCH(R)
71	3050 (3.4)	3045 (<1)	3049 (<1)	n.o.	νCH(r)
72	3163 (25.8)	3140 (43.7)	3179 (51.1)	3136 (m)	ν_s NH_3^+
				3215 (m)	
73	3252 (88.1)	3251 (81.2)	3255 (89.5)	3267 (vs)	ν_{as} NH_3^+
74	3339 (61.3)	3361 (23.4)	3347 (24.7)	3336 (vs)	ν_{as} NH_3^+
75	3439 (88.6)	3436 (68.2)	3438 (59.8)	3387 (vs)	νNH(r)

[a] Scaled vibrational SCRF frequencies at the level HF/6-31(d,p) for the three conformers: G$^+$, G*, and G. The relative intensities (in parentheses) for all predicted bands are arbitrarily scaled such that the strongest intensity in each spectrum is 100. [b] Observed IR spectral bands obtained by DSD method. The intensities (in parentheses), are qualitatively described as vvs, very very strong; vs, very strong; s, strong; m, medium; w, weak; vw, very weak; sh, shoulder; n.o., not observed. [c] Only group vibrations with largest contributions are presented: ν, stretching; β, bending; def., deformation; s, symmetric; as, asymmetric; R, benzene ring; r, pyrrole ring.

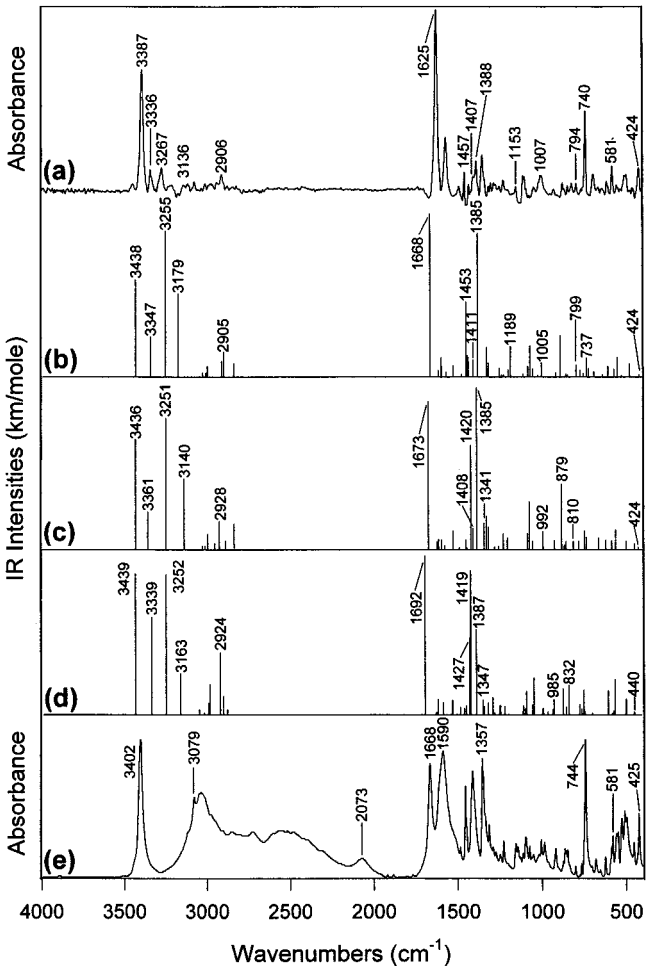

Figure 3. Mid-IR spectra of zwitterionic Trp obtained by different methods: (a) DSD; SCRF/HF predictions for conformers G (b), G* (c), and G$^+$ (d), respectively; (e) KBr pellet.

The question of whether a particular conformer is predominant in the prepared DSD sample, and its identification, can be elucidated by careful comparison of the calculated vibrational frequencies and intensities for each of the three conformers, with the observed bands in the DSD spectrum. There are a total of 75 fundamental vibrational modes for Trp, 63 modes of which (ν_{13} to ν_{75}) have frequencies within the range 400−4000 cm^{-1}. Cursory inspection of the calculated spectra in Figure 3 for the three conformers does not highlight major differences among them. However, careful and detailed examination of some modes, in particular numbers 18, 27, 35, 43, 51, 52, 53, 56, 63, and 66, reveals significant differences in the predicted spectra of the three conformers, either in frequencies, intensities, or both. These differences are significant because they relate directly to conformational differences. For convenience of comparison, these 10 modes have been listed in a separate Table 2, together with the corresponding DSD observed bands. In addition, the differences between the predicted and observed frequencies ($\Delta\nu = \nu_{SCRF} - \nu_{DSD}$, cm^{-1}) are also listed in the table.

The comparison of the scaled vibrational frequencies and intensities can be best examined by dividing the observations into three categories according to the magnitude and nature of the differences. In the first category, the DSD bands are not observed (n.o.) at all (modes 18 and 51), while the predicted intensities of these bands are seen to display (Table 2) large differences. The calculated frequencies of these two modes for the three conformers are very close. However, only for conformer G are the intensities (I) of these two modes in

TABLE 2: Comparisons of the Vibrations Most Sensitive to Conformational Changes (cm^{-1})

	G^+		G*		G		DSD
no.	ν (int.)	$\Delta\nu$	ν (int.)	$\Delta\nu$	ν (int.)	$\Delta\nu$	ν (int.)
18	567 (2.4)		560 (2.6)		561 (<1)		n.o.
51	1347 (9.1)		1341 (16.4)		1340 (<1)		n.o.
43	1184 (<1)	+31	1181 (<1)	+28	1189 (18.8)	+36	1153 (m)
53	1419 (90.4)	+12	1408 (13.1)	+1	1411 (10.4)	+4	1407 (w, sh)
56	1457 (4.2)	0	1450 (5.9)	−7	1453 (46.1)	−4	1457 (s)
52	1387 (53.6)	−1	1385 (100)	−3	1385 (88.2)	−3	1388 (vs)
63	1692 (100)	+67	1673 (91.3)	+48	1668 (100)	+43	1625 (vvs)
27	832 (18.5)	+38	810 (5.2)	+16	799 (7.3)	+15	794 (w)
35	985 (4.1)	−22	992 (11.3)	−15	1005 (8.8)	−2	1007 (m)
66	2924 (39.0)	+18	2928 (17.7)	+22	2905 (15.5)	+1	2906 (m)

accordance with the observed bands. For the G^+ and G* conformers, appreciable intensities for both modes are predicted by the calculations, particularly for mode 51.

The second category differs from the first in that the corresponding bands in the DSD spectrum have measurable intensities. Modes 43, 52, 53, 56, and 63 belong in this category. For mode 43, only the intensity of conformer G ($I_G = 18.8$) is close to the measured moderate intensity of the band at 1153 cm^{-1} in spectrum a. The absorption intensities for this mode of conformers G^+ and G* are both less than 1, which is far less than the observed moderate intensity. For modes 53 and 56, the predicted frequencies for all three conformers are close to the observed bands ($\Delta\nu = 12, 1, 4$ cm^{-1} for mode 53, and $\Delta\nu = 0, -7, -4$ cm^{-1} for mode 56, respectively), but only the intensities of conformer G agree well with the observed bands. For mode 53, $I_{G^+} = 90.4$, $I_{G^*} = 13.1$, and $I_G = 10.4$, while the observed band (at 1407 cm^{-1}) is weak. For mode 56, $I_{G^+} = 4.2$, $I_{G^*} = 5.9$, and $I_G = 46.1$, and the observed band (at 1457 cm^{-1}) is strong. For modes 52 and 63, their relative intensities help in distinguishing among the conformers. These two modes, located at 1388 and 1625 cm^{-1}, respectively, are among the strongest bands in the observed DSD spectrum, the latter being the most intense. This agrees with conformers G^+ and G, but excludes conformer G*, since its strongest band is at 1385 cm^{-1}, not at 1673 cm^{-1}. It should also be noted that the predicted frequencies of mode 63 for all three conformers were overestimated by 43, 48, and 67 cm^{-1}, for the G, G*, and G^+ conformers, respectively. This point will be expanded upon below. However, it leaves conformer G showing the best frequency agreement with the observed band.

In the final category are those modes whose predicted absorption intensities for all three conformers are similar, but whose predicted frequencies show marked differences. This category is represented by modes 27, 35, and 66. For mode 27, only conformers G ($\Delta\nu = 15$ cm^{-1}) and G* ($\Delta\nu = 16$ cm^{-1}) are the possible candidates whose modes can match, in terms of frequencies and intensities, the observed weak band at 794 cm^{-1}. For mode 35, the frequency differences for conformers G^+, G*, and G with respect to the observed spectrum, are −22, −15, and −2 cm^{-1}, respectively, showing that conformer G has the best frequency agreement. Similarly for mode 66, the calculated intensities of this mode for the three conformers are comparable, but the vibrational frequency of conformer G agrees best with the corresponding observed band ($\Delta\nu = 1$ cm^{-1} for G, but 18 and 22 cm^{-1} for G^+ and G*).

In summary, the SCRF calculated frequencies and intensities for most modes are similar for all three conformers, except for the 10 modes specified in Table 2. The differences in frequencies, and/or intensities, of these 10 modes for the three conformers are instrumental in elucidating which conformer(s) is present in the DSD prepared sample. The detailed comparisons between the predicted and observed frequencies and intensities of these 10 modes have given a consistent conclusion that conformer G is the favored form of Trp in the sample prepared by the DSD technique. However, it should be noted that this conclusion is reached on the assumption that the selection of corresponding bands for the three conformers is correct.

TABLE 3: Comparisons of HF Optimized and MP2 Single-Point Energies for Three Different Trp Zwitterionic Conformers

conformer	E(HF, Hartrees)	ΔE (cm^{-1})	E(MP2, Hartrees)	ΔE (cm^{-1})
G	−681.986031	0	−684.277706	0
G*	−681.986069	−8.3	−684.276696	+221.6
G^+	−681.978010	+1760.4	−684.269507	+1799.4

The above conclusion also receives support from the following energy considerations. Table 3 lists the zero-point corrected SCRF/HF energies and the SCRF/MP2 energies at the SCRF/HF optimized structures for the three conformers of Trp. For SCRF calculations, the system stability is indicated by the total energy which includes solvent energy. It can be seen from Table 3 that conformers G and G* are energetically the most favorable. For the HF calculation, the two are of similar energy, but for the MP2 calculation, the G conformer is clearly favored.

Spectra. In this section, we focus on certain aspects of the infrared spectra of zwitterionic tryptophan, namely the mutual agreement between the predicted and observed spectra, the assignment of the infrared bands, and the comparisons of some key bands in spectra obtained by different methods. The detailed comparisons of the spectra discussed above led us to conclude that conformer G is the most favored in the DSD sample, although contributions to the DSD spectrum from other conformers could not be ruled out. Accordingly, the calculated spectrum of Trp used for discussion in the following is confined to that of conformer G.

The infrared spectrum of Trp obtained by the DSD technique has the following features in common with the DSD spectra of Ala,[33] Phe,[34] Leu,[42] Ile,[42] and Met.[42]

First, in distinction to the KBr pellet spectra (see Figure 3e), there are no bands in the region of 2750−1750 cm^{-1} in the DSD spectrum. In Figure 3a, the two bands closest to this region are at 2816 (w) and 1625 (vvs) cm^{-1}, respectively. This remarkable feature agrees well with the SCRF predicted spectrum in the continuum of KBr; the corresponding two predicted bands are at 2844 and 1668 cm^{-1}, and no other fundamental was predicted between these two bands. In the same region of the Trp KBr pellet spectrum (Figure 3e), a broad absorption contour extends from below 2000 to beyond 3000 cm^{-1}, with distinct structure at 2073 cm^{-1}, and at some higher frequencies. This absorption region appears to be formed from a number of overlapped and broad bands. It is a feature common to KBr pellet spectra of most solid samples, particularly amino acids and nucleic acid bases. The broad absorption has its origin in the strong hydrogen-bonding network present in the tiny crystals (large multimers) that are characteristic of the KBr pellet sample. The differences in this region between the DSD and KBr pellet spectra demonstrate that the DSD technique is able to dilute and separate the sample molecules to a much larger extent than occurs in the normal KBr pellet sample. For Trp in the DSD sample, the zwitterions are mainly present as monomers.

Second, in common with Ala[33] and Phe,[34] three intense bands are predicted by SCRF calculations on Trp zwitterionic monomers in the region of 3400−3100 cm^{-1}. Their frequencies are

3347, 3255, and 3179 cm^{-1} with large or very large relative intensities. This prediction again agrees with the observed DSD spectrum; in Figure 3a, three bands at 3336, 3267, and 3136 cm^{-1} are evident. Two of them have comparable intensities, only the band at 3136 cm^{-1} is relatively weak. This contrasts the KBr pellet spectrum (e) of Trp. No band appears in this region because of the intermolecular hydrogen bonding and the presence of large multimers of Trp zwitterions. The above dramatic differences are very similar to those found between the traditional matrix isolation (MI) and KBr pellet spectra of many solid samples. For example, in the MI spectra of purine[46] and uracil,[47] strong bands at 3485 cm^{-1} for purine and 3493 cm^{-1} for uracil are present as the result of matrix isolation (monomers). These bands are attributed to the NH stretching mode, and were also predicted by SCF calculations (for isolated molecules). However, in the normal KBr pellet spectra, no band appears at a frequency greater than 3100 cm^{-1} for purine and 3200 cm^{-1} for uracil, a consequence of molecular association (multimers).

The final observation of the DSD spectra for zwitterionic amino acids is concerned with the strongest band at around 1630 cm^{-1} (1625 cm^{-1} for Trp). The band is assigned to the asymmetric stretching of the anionic carboxyl group $-CO_2^-$. It has a frequency typically in the region 1650−1600 cm^{-1}. Our SCRF calculations on Ala, Phe, and Trp (G conformer) all show that this band has the largest intensity, which is in accordance with their DSD spectra. In the KBr spectrum (e) of Figure 3, a strong band observed at 1668 cm^{-1} may possibly be assigned to the $-CO_2^-$ group. But it is not the strongest.

In summary, the above features of the DSD spectrum that help to discriminate among the conformers of zwitterionic Trp agree well with the SCRF predictions, and the overall agreement between the DSD and SCRF predicted spectra is evident in Figure 3 and Table 3. The assignments of all the bands in the measurable range of this work has been achieved on the basis of frequency and intensity comparisons of the observed bands with the calculated spectrum and examination of the normal coordinates. The qualitative descriptions (stretching, bending, etc.) of the vibrations have been established from inspection of the normal coordinates expressed in Cartesian coordinates and with the assistance of an interactive visualization molecular orbital program (Molden), which dynamically illustrates the vibrational modes produced by molecular orbital calculations. It is found that, except for a few modes, most vibrations must be described in terms of a substantial mixture of a number of group vibrations. For simplicity, only the major components have been detailed in Table 3. In the following, the frequencies, intensities, and assignments of several of the key bands in the Trp spectra are discussed in detail.

$-CO_2^-$ Group. The band with the largest intensity is located at 1625 cm^{-1} in the DSD spectrum and may be described as largely asymmetric stretching of the $-CO_2^-$ group. This band is very characteristic of the zwitterionic form of the amino acids, since it shows clearly that the carboxyl group of Trp is present as the ionized $-CO_2^-$ and not the unionized form −COOH. For the unionized group −COOH, two strong bands would be expected, one from carbonyl (C═O) stretching in the region 1790−1760 cm^{-1},[31,32,48] and the other from OH stretching at about 3560 cm^{-1}.[31,32,48] In the DSD spectrum of Trp, only one band at 1625 cm^{-1} is observed and no band appears in the region beyond 3500 cm^{-1}. The SCRF calculation placed this band at 1668 cm^{-1} for conformer G with a 43 cm^{-1} overestimation. The frequency overestimation for this band is not unexpected since it is also encountered in other studies. For example, in the MI (Ar matrices) spectra of alanine,[48] which is present in the unionized neutral form, the C═O stretching band is observed at about 1774 cm^{-1} (multiline bands). The SCF calculation at the HF/6-31G(d) level predicted this band at 1805 cm^{-1}, which is an overestimation by 31 cm^{-1}. This magnitude of overestimation is also common for the NH stretching modes, discussed below.

Indole NH Band. The indole NH stretching band (N15−H23), located at 3387 cm^{-1} in the DSD spectrum, is also very strong. The band is of particular interest because its frequency in the DSD spectrum is shifted down by about 15 cm^{-1} compared with its frequency in the KBr pellet spectrum. This is contrary to the usual behavior, where the NH band shifts to higher frequency as the sample molecules are more separated by matrices. The decrease in frequency can be explained by two observations. First, X-ray crystal structure studies[21] of crystal L-tryptophan hydrochloride show that the NH bond in the indole ring does not participate in hydrogen bonding in the solid state. Thus, in the absence of hydrogen bonding, the NH stretching frequency is not lowered in the solid state. From this point of view, the moiety N−H behaves like in the gaseous state. Second, previous SCF and SCRF calculations for purine[33] have shown that the NH stretching band will shift down about 17 cm^{-1} from gas state to solvated state (KBr continuum).

The SCRF prediction for the indole ring NH stretching frequency is overestimated by 51 cm^{-1}. This overestimation is similar to that found for the NH stretching mode of purine, where the observed band is located at 3493 cm^{-1} in the MI spectrum[46] and the predicted value at the HF/6-31G(d,p) level is 3528 cm^{-1}.

$-NH_3^+$ Bands. Three resolved bands (3336, 3267, and 3136 cm^{-1}), attributed to the N−H asymmetric and symmetric stretching vibrations of the cationic amino group $-NH_3^+$, are evident in the DSD spectrum. These bands, particularly the former two, are characteristic of IR spectra of amino acids in monomeric zwitterion forms. They can be used as an index of the extent of matrix isolation, since in the KBr pellet spectrum of Trp no band appears in this region and the band with the highest frequency is only located at 3079 cm^{-1}. Moreover, good agreement exists with the SCRF predicted frequencies, 3347, 3255, and 3179 cm^{-1}, and to a lesser extent intensities, which are overestimated by the calculation, particularly for the band at 3136 cm^{-1}. Similar overestimation of calculated N−H stretching vibrational intensities can also be found in MI studies of unionized amino acids. For example, for the stretching vibrations assigned to the $-NH_2$ group of unionized alanine,[48] the HF calculation predicted two strong bands at 3392 and 3321 cm^{-1}, but in its MI spectrum, both bands are too weak to be observed.

Indole Ring Bands. Three bands associated with the bending of indole ring CH bonds, or indole ring deformations, have appreciable intensities. In the DSD spectrum, these bands located at 740(ν_{24}), 581(ν_{19}), and 424 cm^{-1}(ν_{13}) are in very close agreement with the frequencies in the KBr pellet spectrum, namely 744, 581, and 424 cm^{-1}, and both sets match well the SCRF predicted frequencies of 737, 574, and 424 cm^{-1}, respectively. Nevertheless, when both intensities and frequencies are considered, the DSD bands show somewhat better agreement with the SCRF predictions (Figure 3). Furthermore, it is apparent in Figure 3 that, because of the matrix effect (reaction field), the three bands are shifted to slightly lower frequencies in the DSD spectrum compared to the KBr spectrum. The small red shifts of these bands are usual for bands originating from the motions of nonpolar, saturated, and stable groups. In this

TABLE 4: SCRF Predicted Geometry of Zwitterionic L-Trp (G, this work) and the Crystal Structure of L-Trp·HCl Obtained by X-ray Diffraction Studies[21,49]

bond lengths (Å)			in-plane angles (deg)			dihedral angles (deg)		
bonds	SCRF	X-ray	atoms involved	SCRF	X-ray	atoms involved	SCRF	X-ray
C2−O1	1.2414	1.325	O1−C2−O3	127.897	127.5	C4−C2−O1−O3	177.683	
O3−C2	1.2327	1.147	C4−C2−O1	116.084	125.7	H5−C4−C2−O1	−108.571	
C4−C2	1.5590	1.540	C4−C2−O3	115.982	106.8	N6−C4−O1−O3	−176.266	
H5−C4	1.0830	1.030	H5−C4−C2	107.470		N6−C4−C2−O1 (Ψ^1)	5.081	
N6−C4	1.5099	1.505	N6−C4−C2	108.478	107.0	N6−C4−C2−O3 (Ψ^2)	−176.954	
H7−N6	1.0076	0.990	H7−N6−C4	112.386		H7−N6−C4−C2 (Φ^1)	−132.312	
H8−N6	1.0122	1.020	H8−N6−C4	106.455		H8−N6−C4−C2 (Φ^2)	−10.464	
H9−N6	1.0154	1.100	H9−N6−C4	112.496		H9−N6−C4−C2 (Φ^3)	110.234	
C10−C4	1.5454	1.539	C10−C4−C2	116.499	115.0	C10−C4−C2−O1	129.551	
H11−C10	1.0836	1.040	H11−C10−C4	106.503		H11−C10−C4−C2	72.342	
H12−C10	1.0884	1.050	H12−C10−C4	108.588		H12−C10−C4−C2	−41.980	
C13−C10	1.5070	1.530	C13−C10−C4	113.459	114.2	C13−C10−C4−C2	−164.109	
C14−C13	1.3650	1.344	C14−C13−C10	128.473	128.0	N6−C4−C10−C13 (X^1)	−40.324	65.9
N15−C14	1.3503	1.377	N15−C14−C13	110.452	111.5	C4−C10−C13−C14 ($X^{2,1}$)	−90.658	80.7
C16−N15	1.3717	1.391	C16−N15−C14	109.565	107.4	C4−C10−C13−C17 ($X^{2,2}$)	86.221	−106.7
C17−C16	1.4009	1.382	C17−C16−N15	107.502	107.8	C10−C13−C14−C17	177.364	
C17−C13	1.4499	1.451	C13−C17−C16	106.653	107.7	N15−C14−C13−C10	176.840	
C18−C17	1.4088	1.412	C18−C17−C16	118.606	121.1	C16−N15−C14−C13	0.142	
C19−C18	1.3771	1.397	C19−C18−C17	118.650	114.6	C17−C16−C15−C14	0.320	
C20−C19	1.4065	1.386	C20−C19−C18	121.508	124.8	C18−C17−C16−N15	179.622	
C21−C20	1.3744	1.399	C21−C20−C19	121.071	119.7	C19−C18−C17−C16	0.700	
C21−C16	1.3970	1.400	C16−C21−C20	117.234	116.4	C20−C19−C18−C17	−0.427	
H22−C14	1.0724	1.030	C17−C16−C21	122.925	123.2	C21−C20−C19−C18	−0.260	
H23−N15	0.9985	1.090	H22−C14−C13	129.505		H22−C14−C13−N15	179.603	
H24−C21	1.0764	1.060	H23−N15−C14	125.741		H23−N15−C14−C16	178.286	
H25−C20	1.0749	1.130	H24−C21−C16	121.905		H24−C21−C16−C20	−179.991	
H26−C19	1.0758	1.000	H25−C20−C19	119.791		H25−C20−C19−C21	−179.440	
H27−C18	1.0832	1.070	H26−C19−C18	120.075		H26−C19−C18−C20	−178.967	
			H27−C18−C17	121.227		H27−C18−C17−C19	−176.741	

instance, the group vibrations are associated with the indole ring. This observation gives further credence to the conclusion made in the study of phenylalanine[34] that the reaction field effects are concentrated on the main chain and not the side chains of zwitterionic amino acids with nonpolar side chains.

Finally, it should be pointed out that the assignments proposed for two prominent bands in the ultraviolet resonance Raman (UVRR) spectrum[23,24] of Trp are different from the above. The two bands at 1622 and 1578 cm^{-1} were assigned to benzene vibrational modes ν_{8a} and ν_{8b}[23,24] on the basis of comparison with the assignment of the indole vibrational spectrum. In our DSD infrared absorption spectrum, we propose that from comparison with the SCRF calculations the two strong bands seen at 1625 and 1569 cm^{-1} should be assigned to vibrations of the main chain, that is, $-CO_2^-$ and $-NH_3^+$ groups, respectively. The SCRF calculations also reveal that two further bands corresponding to the benzene vibrational modes ν_{8a} and ν_{8b} occur at similar frequencies to the two seen in the UVRR spectrum. However, we suggest that because of their small predicted absorption intensities they are not seen in our DSD spectrum. Our interpretation also receives support from SCRF calculations carried out on glycine[41] where low Raman activities are obtained for the corresponding vibrations of the $-CO_2^-$ and $-NH_3^+$ groups, explaining their absence in the UVRR work.

Structure. No detailed geometries for isolated neutral Trp were found in the literature. Information about the geometries of the different conformers of its analogue, tryptamine, has been obtained by Levy's group[11,12] from analysis of the rotational structure observed in electronic spectroscopy of supersonic jets. Sulkes et al.[16] used a molecular mechanics method to predict the geometries of jet-cooled conformers of a number of tryptophan analogues, albeit with mixed success. However, insofar as comparisons with the geometry of Trp are concerned, significant structural differences can be expected between tryptamine and Trp and even between the neutral and zwitterionic forms of Trp. This is illustrated by experimental and theoretical studies on alanine; 13 conformers have been located by ab initio calculations on its neutral form,[29] and only one conformer was found for its zwitterionic form.[33]

The crystal structures of Trp hydrochloride and hydrobromide salts have been determined by X-ray diffraction.[21] It should be noted that, in these salts, Trp is essentially present as a positive ion, not a neutral zwitterion. Therefore, our SCRF calculations have provided the only information on the detailed molecular structure of zwitterionic Trp in our DSD samples. The bond lengths and in-plane and dihedral angles of the G conformer, shown above to be the most stable, are compiled in Table 4. In the following, we report on a structural comparison between zwitterionic Trp and its closest analogues, Trp·hydrohalides, L-tyrosine (Tyr), and Tyr·HCl. Since the conformation and structure of the two Trp·hydrohalides is essentially the same,[21] reference is accordingly limited to one, Trp·HCl, in the following discussion.

For zwitterionic amino acids with nonpolar, stable side chains (e.g., Gly, Ala, Val, Leu, Ile, Phe, Trp, etc.), significant structural differences can be expected to exist in the main chain, and not the side chain, for different physical states of the amino acids.[34]

Indole Ring. The side chain indole ring of Trp is not involved in hydrogen bonding in the solid state, nor is it associated with HCl to form the hydrohalide salts.[21] Consequently, the structures of the indole ring for Trp in the crystal state or in the solvated state should be very similar. This is illustrated in Table 4. The bond lengths and in-plane angles of the indole ring predicted by the SCRF calculation are very close to those determined by X-ray diffraction of Trp·HCl in the crystal state. The SCRF predicted average C−C bond distances of the pyrrole and benzene rings of Trp are 1.388 and 1.394 Å, respectively, compared to 1.389 and 1.396 Å in the crystal state by X-ray diffraction of Trp·HCl.[21] The average C−H bond distances on

TABLE 5: Comparisons of Dihedral (Torsion) Angles (deg) for the Three Predicted Conformers (G^+, G*, G) of Zwitterionic Trp, with X-ray, (Trp·HCl), and Neutron Diffraction (Tyr and Tyr·HCl) Results

angles	atoms involved	Trp (G^+)[a]	Trp (G*)[a]	Trp (G)[a]	Trp·HCl[b]	Tyr[c]	Tyr·HCl[c]
X^1	N6−C4−C10−C13	+37.851	−45.547	−40.324	+65.9	+69.1	−178.1
$X^{2,1}$	C4−C10−C13−C14	−108.459	+116.430	−90.658	+80.7	−86.0	−113.6
$X^{2,2}$	C4−C10−C13−C17	+85.268	−62.037	+86.221	−106.7		
Ψ^1	N6−C4−C2−O1	+13.897	−7.978	+5.081		−14.2	−31.8
Ψ^2	N6−C4−C2−O3	−170.316	+171.826	−176.954		+166.3	+151.1
Φ^1	H7−N6−C4−C2	−138.515	−103.751	−132.312		+57.0	+47.1
Φ^2	H8−N6−C4−C2	−16.323	+16.438	−10.464		+177.0	+167.8
Φ^3	H9−N6−C4−C2	+101.108	+138.223	+110.234		−62.4	−72.2

[a] SCRF calculations of this work. [b] X-ray diffraction.[21,49] [c] Neutron diffraction.[50]

the indole ring are also in agreement, 1.064 Å by SCRF and 1.047 Å by X-ray diffraction with 0.015 Å average standard deviation.

The conformation and relative orientation of the indole ring can be described by three dihedral or torsion angles, namely X^1, $X^{2,1}$, and $X^{2,2}$ defined in Table 5. The SCRF calculated torsion angles for the three predicted Trp conformers and the X-ray results[21,49] for the Trp·HCl salt are listed in Table 5, together with several other relevant torsion angles. For comparison, the corresponding torsion angles of L-tyrosine (Tyr) and Tyr·HCl are also included in the table, since they have been fully determined by neutron diffraction studies.[50] The IUPAC−IUB conventions[50] have been adopted to denote these torsion angles.

Marked conformational differences involving the indole ring are found between Trp zwitterion and Trp·HCl salt. The three torsion angles for the G conformer of Trp are by calculation −40.3°, −90.7°, and 86.2°, respectively, while for Trp·HCl, these torsion angles found by X-ray diffraction are 65.9°, 80.7°, and −106.7°. This conformational difference can be seen more clearly in Figure 2, where the stereographic projections about the C4−C10 ($C_\alpha-C_\beta$) bond are given for the three SCRF predicted conformers (a, b, c), and X-ray structure (d) of Trp·HCl. With respect to the NH_3^+ group, the predominant SCRF conformer G (Figure 2a) indicates a gauche$^-$ form, while the X-ray structure of Trp·HCl (Figure 2d) is in the gauche$^+$ form. Both conformations were found in Trp derivatives: *N*-acetyl-L-tryptophan(g^-)[51] and DL-tryptophan ethyl ester hydrochloride (g^+).[52] Moreover, this conformational difference is not unique to Trp. It has also been observed for Tyr and Tyr·HCl by neutron diffraction studies;[50] the former (Tyr) is in the g^-, while the latter is in the g^+ form. The torsion angle of C10−C13−C14−C17 for the G conformer is predicted to be 176.9° ($X^{2,2}-X^{2,1}$). Its value clearly indicates that the atoms of C10, C13, C14, and C17 are nearly coplanar, and this is also the case found in the crystal structures of Tyr and Tyr·HCl.[50]

Anionic Carboxyl Group. In the zwitterionic Trp, the carboxyl group $-CO_2H$ is ionized to $-CO_2^-$ and the two CO bond lengths are expected to be similar. This is confirmed by the SCRF calculation, which gave 1.2414 and 1.2327 Å. However, in the Trp·HCl salt, the carboxyl is present as the neutral $-CO_2H$ group, and so the two −CO bond distances should be quite different, in agreement with the X-ray diffraction results of 1.325 and 1.147 Å (Table 4).[21] The average CO bond length difference ($\Delta(CO_1 + CO_2)/2$) between $-CO_2^-$ (SCRF) and $-CO_2H$ (X-ray) is about 0.001 Å. In the crystal structures of (Tyr) and its hydrochloride salt (Tyr·HCl), these two CO bond distances were found by neutron diffraction[50] to be 1.259, 1.242 Å, and 1.304, 1.205 Å, respectively. Their average bond length difference is 0.004 Å, which is similar to that of Trp in this work. The in-plane angles between the two CO bonds in Trp zwitterion and Trp·HCl salt are very close, 127.9° (SCRF) and 127.5° (X-ray), respectively. Similarly for Tyr and Tyr·HCl, the angles between the two CO bonds are found to be the same, 126.4°.[50] Finally, according to the SCRF calculation, the torsion angle formed by N6, C4, O1, and O3 in Trp is found to be −176.3°, which indicates that the four atoms are nearly coplanar. This is also the case found in the X-ray crystal structures of Tyr and Tyr·HCl. For the crystal structure of Trp·HCl, the X-ray studies[21] did not give sufficiently detailed information to allow determination of this angle.

Cationic Amino Group. The amino group is protonated as $-NH_3^+$ in both zwitterionic Trp and Trp·HCl salt. The SCRF predicted bond distances of the three N−H bonds in $-NH_3^+$ for the Trp G conformer are 1.008, 1.012, 1.015 Å, respectively. In the X-ray studies of Trp·HCl,[21] these bond lengths were determined to be 0.990 (0.11), 1.020 (0.16), and 1.100 (0.13) Å with large standard deviations (in parentheses, Å). The considerable discrepancies in the NH bond lengths of the $-NH_3^+$ group between the SCRF predictions and X-ray studies can be ascribed to two factors. First, the X-ray diffraction method is usually not able to determine accurate positions of hydrogen atoms. Second, in the crystal of Trp·HCl, the cationic amino group is hydrogen bonded to the neighboring negative ions. This interaction is different from that in the DSD prepared sample, in which a uniform reaction field is believed to describe the interaction between the solute (Trp zwitterions) and the solid solvent (KBr matrix). Therefore, the structures and conformations of the $-NH_3^+$ group in the crystal state and in the SCRF reaction field are essentially different from each other. This difference is also seen in a comparison of the torsion angles (Φ^1, Φ^2, Φ^3, in Table 5) of the $-NH_3^+$ group, between Trp zwitterions (SCRF) and Trp·HCl salt (X-ray). For example, one hydrogen atom in the $-NH_3^+$ group of Trp·HCl is in a trans position with respect to C2, according to the figure presented,[21] while for Trp zwitterions this hydrogen is at an eclipsed position ($\Phi^2 = -10.464$).

Conclusions

The infrared spectra and molecular structure of zwitterionic Trp were obtained by means of a new infrared sampling technique (DSD) and SCRF ab initio molecular orbital calculations in the continuum of KBr. Only three conformers of Trp zwitterions were found by the SCRF calculations. One of them was determined to be the dominant and most stable conformation in the DSD sample. Good agreement was established between the calculated spectrum (conformer G) and the observed DSD spectrum, although spectral differences for the three conformers are subtle. The detailed molecular structure and conformation of zwitterionic Trp (G conformer) was obtained and compared with the X-ray crystal structure of its closest analogues. Considerable structural differences were found between Trp zwitterion in a solid solvent of KBr and its hydrochloride salt,

and they have been ascribed to the marked differences of their local environments.

Substantial differences were found between the DSD and KBr pellet spectra of Trp. They have been related to the extent of matrix isolation. In analogy with Ala and Phe, this study shows that the KBr pellet spectra of zwitterionic amino acids are inappropriate for direct comparison with the spectra predicted by ab initio molecular calculations performed on single molecules. For the meaningful prediction of the spectra and structure of zwitterionic amino acids, SCRF methods and appropriate continua must be used. In addition to their existence in solution and crystals, the zwitterions of Trp can also exist in the KBr matrix (solid solvent) prepared by the DSD method. In this matrix, the largely monomeric zwitterions are stabilized by the reaction field between the solute and the solid solvent.

Acknowledgment. The Australian Research Council is thanked for its support of this work. The ab initio calculations were carried out on the Fujitsu VPP and the Silicon Graphics Power Challenge of the ANU Supercomputer Facility. XLC is indebted to the Australian National University and the Australian Government for the award of scholarships. We also thank Dr. Rob Stranger, David Smith, and Damien Kuzek for their help in molecular modeling programs and useful discussions.

References and Notes

(1) Chang, M. C.; Petrich, J. W.; McDonald, D. B.; Fleming, G. R. *J. Am. Chem. Soc*. **1983**, *105*, 3819.
(2) Willis, K. J.; Szabo, A. G.; Kracjarski, D. T. *Chem. Phys. Lett.* **1991**, *182*, 614.
(3) Anderson, J. S.; Bowitch, G. S.; Brewster, R. L. *Biopolymers* **1983**, *22*, 2459.
(4) Rizzo, T. R.; Park, Y. D.; Peteanu, L. A.; Levy, D. H. *J. Chem. Phys*. **1985**, *83*, 4819.
(5) Rizzo, T. R.; Park, Y. D.; Peteanu, L. A.; Levy, D. H. *J. Chem. Phys*. **1986**, *84*, 2534.
(6) Rizzo, T. R.; Park, Y. D.; Peteanu, L. A.; Levy, D. H. *J. Chem. Phys*. **1986**, *85*, 6945.
(7) Philips, L. A.; Webb, S. P.; Martinez, S. J., III; Fleming, G. R.; Levy, D. H. *J. Am. Chem. Soc*. **1988**, *110*, 1352.
(8) Park, Y. D.; Rizzo, T. R.; Peteanu, L. A.; Levy, D. H. *J. Chem. Phys*. **1986**, *84*, 6539.
(9) Philips, L. A.; Levy, D. H. *J. Phys. Chem.* **1986**, *90*, 4921.
(10) Philips, L. A.; Levy, D. H. *J. Phys. Chem.* **1988**, *92*, 6554.
(11) Philips, L. A.; Levy, D. H. *J. Chem. Phys*. **1988**, *89*, 85.
(12) Wu, Y. R.; Levy, D. H. *J. Chem. Phys.* **1989**, *91*, 5278.
(13) Sipior, J.; Sulkes, M.; Auerbach, R.; Boininеau, M, *J. Phys. Chem.* **1987**, *91*, 2016.
(14) Sipior, J.; Sulkes, M, *J. Chem. Phys*. **1988**, *88*, 6146.
(15) Teh, C. K.; Sipior, J.; Sulkes. M. *J. Phys. Chem.* **1989**, *93*, 5393.
(16) Sipior, J.; Sulkes, M, *J. Chem. Phys*. **1993**, *98*, 9389.
(17) Engh, R. A.; Chen, L. X.; Fleming, G. R. *Chem. Phys. Lett.* **1986**, *126*, 365.
(18) Petrich, J. W.; Chang, M. C.; McDonald, D. B.; Fleming, G. R. *J. Am. Chem. Soc*. **1983**, *105*, 3824.
(19) Gordon, H. L.; Jarrell, H. C.; Szabo, A. G.; Willis, K. J.; Somorjai, R. L. *J. Phys. Chem.* **1992**, *96*, 1915.
(20) Dezube, B.; Dobson, C. M.; Teague, C. E. *J. Chem. Soc., Perkin Trans. 2* **1981**, 730.
(21) Takigawa, T.; Ashida, T.; Sasada, Y. *Bull. Chem. Soc. Jpn.* **1966**, *39*, 2369.
(22) Su, C.; Wang, Y.; Spiro, T. G. *J. Raman Spectrosc*. **1990**, *21*, 435−440.
(23) Rava, R. P.; Spiro, T. G.; *J. Phys. Chem*. **1985**, *89*, 1856−1861.
(24) Rava, R. P.; Spiro, T. G. *J. Am. Chem. Soc*. **1984**, *106*, 4062−4064.
(25) Harada, I.; Miura, T.; Takeuchi, H. *Spectrochim. Acta* **1986**, *42A*, 307.
(26) Hirakawa, A. Y.; Nishimara, Y.; Matsumoto, T.; Nakanishi, M.; Tsuboi, M. *J. Raman Spectrosc*. **1978**, *7* (5), 282.
(27) Hu, C. H.; Shen, M.; Schaefer, H. F., III *J. Am. Chem. Soc*. **1993**, *115*, 2923.
(28) Cao, M.; Newton, S. Q.; Pranato, J.; Schafer, L. *J. Mol. Struct. (THEOCHEM)* **1995**, *332*, 251.
(29) Császár, A. G. *J. Phys. Chem*. **1996**, *100*, 3541.
(30) Ding, Y.; Krogh-Jespersen, K. *Chem. Phys. Lett.* **1992**, *199*, 261.
(31) Reva, I. D.; Plokhotnichenko, A. M.; Stepanian, S. G.; Ivanov, A. Y.; Radchenko, E. D.; Sheina, G. G.; Blagoi, Y. P. *Chem. Phys. Lett*. **1995**, *232*, 141.
(32) Reva, I. D.; Plokhotnichenko, A. M.; Stepanian, S. G.; Ivanov, A. Y.; Radchenko, E. D.; Sheina, G. G.; Blagoi, Y. P. *J. Mol. Struct.* **1994**, *318*, 1.
(33) Cao, X.; Fischer, G. *Spectrochim. Acta* **1999**, *55*, 2329.
(34) Cao, X.; Fischer, G. *J. Mol. Struct.*, in press.
(35) Chakraborty, D.; Manogaran, S. *Chem. Phys. Lett.* **1998**, *294*, 56.
(36) Sambrano, J. R.; de Sousa, A. R.; Queralt, J. J.; AndrÈs, J.; Longo, E. *Chem. Phys. Lett*. **1998**, *294*, 1.
(37) Yu, G.; Freedman, T. B.; Nafie, L. A. *J. Phys. Chem*. **1995**, *99*, 835.
(38) Foresman, J. B.; Frisch, *Æ. Exploring Chemistry with Electronic Stucture Methods*, 2nd ed.; Gaussian, Inc.: Pittsburgh, PA, 1996; p 237.
(39) Foresman, J. B. Private communication, Nov. 3, 1998.
(40) *Handbook of Chemistry and Physics*, 78th ed.; Lide, R. C., Ed.; CRC Press LLC: Boca Raton, FL, 1997; pp 7-1, 8-115, 12-51.
(41) Cao, X.; Fischer, G. *Proceedings of the 22nd Annual Meeting of Australian Society for Biophysics*; Australian National University: Canberra, December, 1998.
(42) Unpublished results.
(43) Khawas, B.; Krishna Murti, G. S. R. *Acta Crystallogr*. **1969**, *B25*, 1006.
(44) Frisch, M. J.; Trucks, G. W. ; Schlegel, H. B.; Scuseria, G. E.; Robb, M. A.; Cheeseman, J. R.; Zakrzewski, V. G.; Montgomery, J. A., Jr.; Stratmann, R. E.; Burant, J. C.; Dapprich, S.; Millam, J. M.; Daniels, A. D.; Kudin, K. N.; Strain, M. C.; Farkas, O.; Tomasi, J.; Barone, V.; Cossi, M.; Cammi, R.; Mennucci, B.; Pomelli, C.; Adamo, C.; Clifford, S.; Ochterski, J.; Petersson, G. A.; Ayala, P. Y.; Cui, Q.; Morokuma, K.; Malick, D. K.; Rabuck, A. D.; Raghavachari, K.; Foresman, J. B.; Cioslowski, J.; Ortiz, J. V.; Stefanov, B. B.; Liu, G.; Liashenko, A.; Piskorz, P.; Komaromi, I.; Gomperts, R.; Martin, R. L.; Fox, D. J.; Keith, T.; Al-Laham, M. A.; Peng, C. Y.; Nanayakkara, A.; Gonzalez, C.; Challacombe, M.; Gill, P. M. W.; Johnson, B.; Chen, W.; Wong, M. W.; Andres, J. L.; Gonzalez, C.; Head-Gordon, M.; Replogle, E. S.; Pople, J. A. *Gaussian 98*, revision A.6; Gaussian, Inc.: Pittsburgh, PA, 1998.
(45) Scott, A. P.; Radom, L. *J. Phys. Chem*. **1996**, *100*, 16502.
(46) Nowak, M. J.; Rostkowska, H.; Lapinski, L. J.; Kwiatkowski, S.; Leszczynski, J. *Spectrochim. Acta* **1994**, *50A*, 1081.
(47) Les, A.; Adamowicz, L.; Nowak, M. J.; Lapinski, L. *Spectrochim. Acta* **1992**, *48A*, 1385.
(48) Rosado, M. T. S.; Duarte, M. L. R. S.; Fausto, R. *J. Mol. Struct*. **1997**, *410*−*411*, 343.
(49) Harada, Y.; Iitaka, Y. *Acta Crystallogr*. **1977**, *B33*, 244.
(50) Frey, M. N.; Koetzle, T. F.; Lehmann, M. S.; Hamilton, W. C. *J. Chem. Phys.* **1973**, *58*, 2547.
(51) Yamane, T.; Andou, T.; Ashida, T. *Acta Cryst*. **1977**, *B33*, 1650.
(52) Vijayalakshimi, B. K.; Srinivasan, R. *Acta Cryst.* **1975**, *B31*, 999.